#### SCATTERING MECHANISMS IN (Al,Ga)As/GaAs 2DEG STRUCTURES

J.J. Harris, C.T. Foxon, D.E. Lacklison and K.W.J. Barnham\*

Philips Research Laboratories, Redhill, Surrey, England.

Received 18th August 1986

We have prepared a large number of high mobility two-dimensional electron gas (2DEG) structures, with undoped spacer thicknesses ranging from 9 to 3200Å. For samples with 400Å of (Al,Ga)As Si-doped at  $1.3 \times 10^{18}$  cm $^{-3}$ , there is a peak in the 4K mobility at spacers of  $400-800 \mbox{\sc A}$ , with a maximum value of  $2 \times 10^6$  cm $^2$  V-l s-l. Increasing the thickness of the doped (Al,Ga)As to  $500 \mbox{\sc A}$  produced an increase in mobility to  $3 \times 10^6$  cm $^2$  V-l s-l for a  $400 \mbox{\sc A}$  spacer sample. We have compared these results with published analyses of scattering processes in 2DEG structures, and conclude that a combination of ionised impurity and acoustic phonon scattering gives a qualitative explanation of the behaviour, but that the experimental mobility values are generally higher than those predicted theoretically.

### 1. Introduction

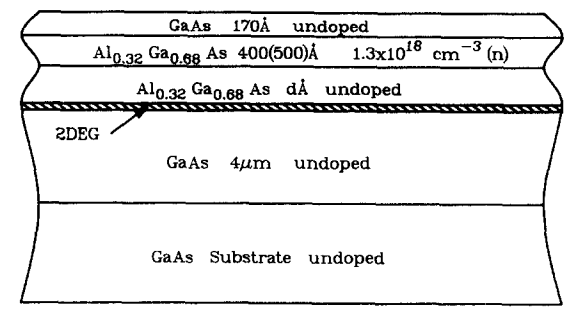
Analysis of the scattering mechanisms in (Al,Ga)As/GaAs two-dimensional electron gas (2DEG) structures has been the subject of a large number of publications, see, e.g. 1-7. When comparison has been made with a limited number of experimental samples, fair agreement has usually been achieved by considering a combination of scattering mechanisms, of which the most important at 4K have been (a) ionised impurity scattering from centres in the doped (Al,Ga)As layer, the undoped spacer layer, the heterojunction interface and the undoped GaAs, and (b) acoustic phonons, via the deformation potential and piezoelectric interactions. The relative importance of these mechanisms will depend on the details of the structure grown and the quality of the component materials, and so in order to elucidate the contributions of the various factors involved, we have used MBE to grow a large number of very high mobility 2DEG layers  $^8$ ,  $^9$ , including a structure with mobility in excess of 3.0x10 $^6$  cm $^2$  V $^{-1}$  s $^{-1}$  at 4K $^9$ . By a systematic study of the effect of varying the thickness of the undoped spacer and of the doped (Al,Ga)As, and by monitoring the clean-up behaviour of the MBE machine, we have been able to show qualitatively how the structural and material parameters influence the mobility in a wide range of samples. However, comparison with existing theoretical models, where appropriate, shows that, in general, our experimental mobilities are significantly greater than predicted, even when account is taken of shallow and deep impurity levels in the doped (A1,Ga)As.

# \* SERC/Royal Society, Industrial Fellow, on leave from Imperial College.

### 2. Experimental

The samples were prepared in a Varian Gen-II MBE machine, and details of the growth process have been reported elsewhere 10. The structures studied are shown schematically in Fig. 1; the thickness, d, of the undoped spacer layer was varied between 9 and 3200Å, and two thicknesses of doped (Al,Ga)As, 400 and 500Å, were used. Electrical measurements were performed on both van der Pauw and Hall bar geometry samples, using alloyed NiAuGe contacts.

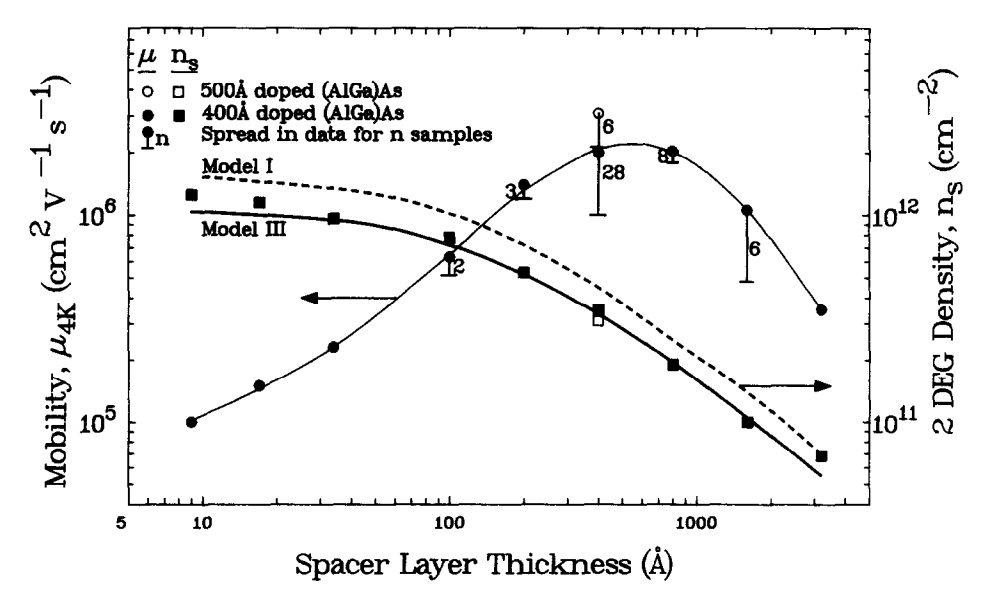
In addition to the samples described above, the clean-up process in the MBE machine was monitored by the occasional growth of thick layers of lightly Si-doped GaAs (n  $\approx 10^{14}\text{--}10^{15}\,\text{cm}^{-3})$  in order to assess the background impurity level from 77K mobility measurements  $^{1}$ l.



 Schematic cross-section of the 2DEG structures studied in this work.

Table I: Properties of lightly-doped GaAs samples as a function of number of layers after reload

Layers after reload	:	1	10	62
$\mu$ 77K, cm <sup>2</sup> V <sup>-1</sup> s <sup>-1</sup>	:	41,000	76,000	100,000
$N_D$ , $cm^{-3}$	:	2.5x1015	8.5x10 <sup>14</sup>	5.5x10 <sup>14</sup>
$N_{A}$ , $cm^{-3}$	:	1.4x1015	4.5x1014	2.1x1014



2. Mobility,  $u_{4K}$ , and sheet charge,  $n_s$ , measured at 4.2K, as a function of undoped spacer thickness, d. The figures against

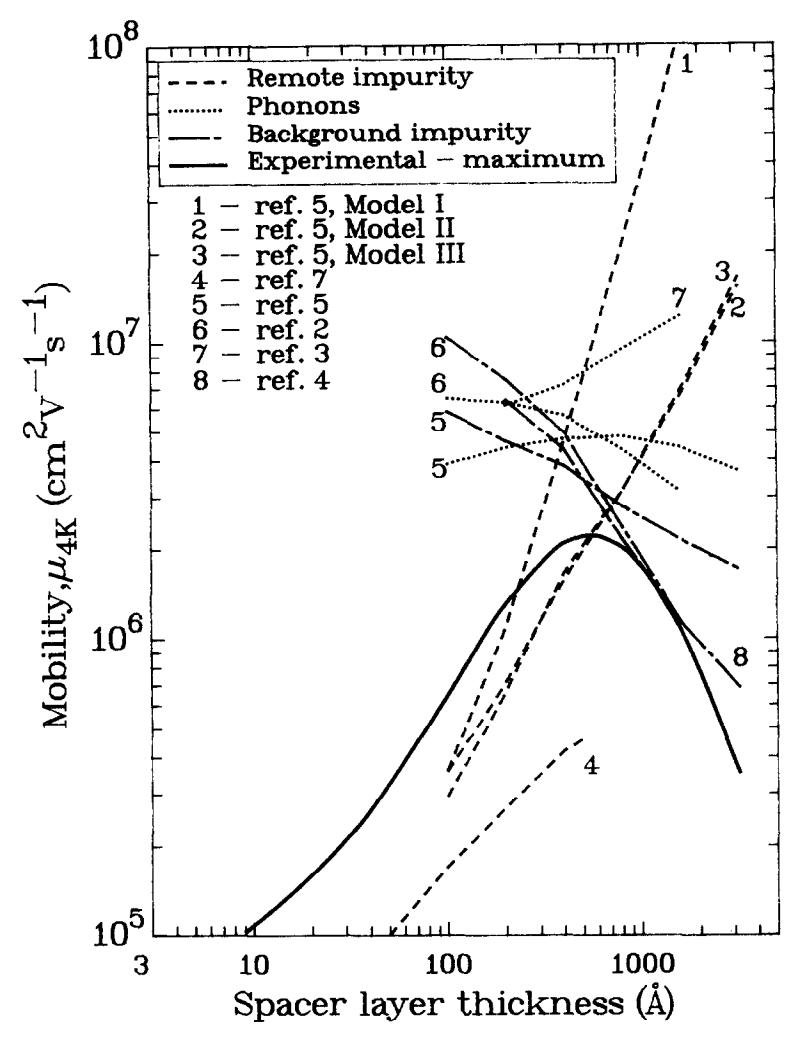
the error bars are the number of samples measured, and the theoretical  $n_{\rm S}{\rm -d}$  curves I and III are discussed in the text.

# 3. Results

There is a gradual improvement in the quality of material from the MBE machine as the number of uninterrupted growth runs increases, following the reloading of the source cells  $^{10}\cdot$ This is illustrated in Table I, where the background acceptor concentration, NA, in lightlydoped GaAs is given as a function of the number of the growth run following a reload. It can be seen that NA rapidly decreased to a value of  $4.5\!\times\!10^{14}$  cm  $^{-3}$  , and then slowly falls to  $\sim$   $2\!\times\!10^{14}$  $cm^{-3}$  over a further 52 layers. This reduction in NA is expected to reduce the amount of scattering by background impurities in the GaAs region of the 2DEG structures, but there is some evidence to suggest that the quality of the (Al,Ga)As is also improving as the run sequence progresses. There is a general trend towards higher mobilities in the repeated growth, at

intervals, of the same 2DEG structures, including those in which background scattering in the GaAs is not thought to be a significant factor. This is most easily explained as being due to a reduction of unintentional scattering centres in the (Al,Ga)As. A similar improvement in the properties of (Al,Ga)As layers, as assessed by optical techniques, has also been observed in other MBE equipment 12.

Clearly, such a gradual change in material quality with time will complicate the analysis of the influence of structural parameters on mobility. However, the samples used in studying the effect of spacer and doped layer thicknesses were all grown at least 10 layers after reload, and in random order; consequently, variations in material quality will be minimised. Furthermore, since several samples were grown for each 2DEG structure, comparison of the maximum mobility obtained for each structure will be most



 Theoretical calculations of mobility limited by remote impurities, background impurities and acoustic phonons at 4.2K, compared with the maximum mobility curve from Fig. 2.

representative of the effects of sample geometry. Additional complications in interpreting low temperature measurements arise from the observation of some dependence of the properties of the layers on light sensitivity and cooling rate. Consequently we have chosen to compare results after saturation of the persistent photoconduction (PPC) effect using a pulse of white light at 4K. The mobility  $\mu_{4K}$  and sheet charge,  $n_{\rm S}$ , in the 2DEG are plotted as a function of spacer layer thickness, d, in Fig. 2, for the two doped (Al,Ga)As thicknesses of 400Å and 500Å. It can be seen that, for the former structures, there is a gradual decrease in  $n_{\rm S}$  with d, and a peak in the mobility of just over 2x106 cm<sup>-2</sup> V<sup>-1</sup> s<sup>-1</sup> for d  $\approx$  400-800Å. Increasing the thickness

of the doped (Al,Ga)As to 500Å produces a considerable improvement in mobility for d=400Å, where a value of 3.09x10 $^6$  cm $^2$  V $^{-1}$  s $^{-1}$  has been achieved.

## 4. Discussion

The qualitative features of Fig. 2 are readily explained by considering two regions of the  $\mu\text{--d}$  curves:

(a) d < 400Å, where the increase in μ with d derives from the increased separation of the remote charged centres in the doped (Al,Ga)As from the 2DEG channel, and

Table II: Parameters used in theoretical calculations

Background doping,  $N_A$  :  $3x10^{14}$  cm<sup>-3</sup>

(A1,Ga)As doping level,  $N_D$ : 1.3x10<sup>18</sup> cm<sup>-3</sup>

Dielectric constant,  $\varepsilon$ : 13.18-3.12x

where x = aluminium fraction (0.33)

Deformation potential, D : 7 (Lee, Walukiewicz)

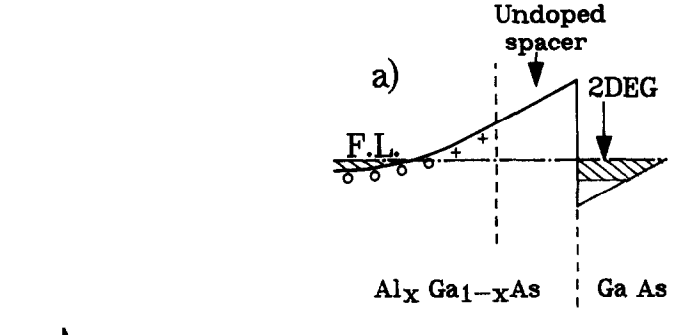
or 13.5 (Price) eV

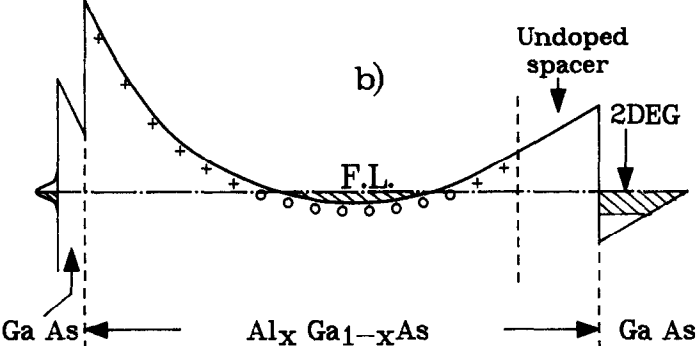
(b) d > 800Å, where the reduction of mobility is the result of the  $n_s$ -dependence of the geometry-independent scattering mechanisms, i.e. background impurities and acoustic phonons. It should be noted that, although the observed decrease of  $\mu$  with decreasing ns is predicted for ionised impurity and piezoelectric3 scattering, an increase in u for lower  $n_{\rm S}$  is expected for deformation potential scattering<sup>3</sup>. The  $\mu$ -n<sub>s</sub> behaviour of acoustic phonon scattering will be determined by a combination of the two interaction mechanisms, and consequently our data can only be explained by acoustic phonon scattering if the piezoelectric interaction is the dominant mechanism. Since phonon scattering is largely independent of material quality, the observation of a higher peak mobility at a wider spacer thickness than previously reported 13 probably reflects a lower background impurity concentration in our material; even so, it is not possible on this evidence to determine whether phonons or background impurities dominate in our samples.

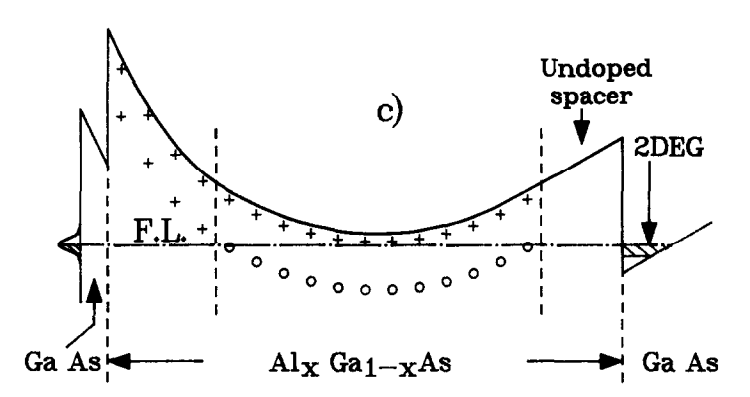
We have attempted a quantitative comparison of our mobility data with some of the theoretical calculations which have appeared in the literature2-5,7. Unfortunately, the more comprehensive models have generally required numerical analysis, and only a limited number of results can be directly applied to our data because the model parameters used do not correspond to our structures. However, in some cases it is possible to scale the calculated results, and by this technique we have generated theoretical curves for mobility limited by remote impurities, background impurities and acoustic phonons, as shown in Fig. 3. The curves labelled I, II and III are derived from the analytic expressions of Lee et al.5, and will be discussed more fully below; the parameters used in these and the other calculations are listed in Table II, and the  $n_{\rm S}$  value for each spacer thickness was taken from Fig. 2. Two important points are apparent from Fig. 3:

(a) there is a considerable difference in the quantitative results of the various calculations, and (b) when these various curves are combined into a total mobility resulting from all three scattering mechanisms, the results are generally significantly lower than is observed experimentally, and the discrepancy would be aggravated by the inclusion of other possible mechanisms, e.g. charge in the undoped spacer, or interface effects, such as roughness, localisation or interface charge.

In order to try and clarify the dependence of mobility on sample dimensions (i.e. doped and undoped (Al, Ga) As thicknesses) we have applied the formulae of Lee et al. 5 to three models of the charge distribution in a 2DEG structure corresponding to the curves I, II and III of Fig. 3. Model I (Fig. 4a) considers scattering due to an interface depletion region in the doped (Al,Ga)As with a space charge density, ND+, equal to the Si doping level, ND. This appears to give a reasonable fit to the experimental data, but is almost certainly wrong, since, in common with most published analyses including those represented here, it fails to take into account the presence of a high density of charged centres in the surface depletion layer of the doped (Al, Ga) As. That such a layer can influence the channel mobility is demonstrated by the fact that using a thicker doped (Al, Ga) As layer, thereby increasing the surface-to-channel separation, results in a considerable increase in mobility (see Fig. 2). This effect has also been predicted theoretically4,6, but to our knowledge this is the first experimental confirmation. Model II (Fig. 4b) has therefore included scattering from this surface depletion region, and it can be seen that a significant reduction in mobility results, so that the agreement with experiment is poor. In an effort to improve the fit with our data, and indeed to use a more realistic model for the doped (Al,Ga)As region, we have considered the effect of the Si dopant giving rise to both shallow and deep levels 14,15. The consequent charge distribution in the 2DEG structure then appears as in Fig. 4c; the exact details depend on the Al content and the sample geometry, and will be reported in detail elsewhere 16, but this distribution forms the basis of model III. can be seen that, with the exception of the 100Å







- 4. Models used to predict  $n_g$ -d variation and remote impurity contributions to scattering as discussed in text:
  - a) Model I: Only heterojunction depletion charge in barrier contributes as in Ref. 5.
- spacer sample, the two curves are extremely close, and the changes to the model are not reflected in an improved fit to the mobility curve. It should be pointed out, however, that the  $n_{\rm S}{}^{-}{\rm d}$  behaviour can be fitted very well by model III, as shown by the theoretical curve III in Fig. 2, whereas models I and II predict  $n_{\rm S}$  values approximately 20% higher (curve I).
- b) Model II: As in a) but with surface depletion charge contribation.
- c) Model III: Both heterojunction and surface depletion charges are separated into deep and shallow levels.

The similarity of the mobility curves II and III arises from two factors which become significant at wider spacer thicknesses, namely (a) the scattering rate from the charges in the surface depletion layer is actually greater than for those in the near-interface depletion region, and (b) the scattering from the latter region becomes only weakly dependent on the effective

doping level in the (A1,Ga)As; these effects will also be considered more fully in a subsequent publication  $^{16}$ .

### 5. Conclusions

We have demonstrated that the gradual improvement in the quality of MBE-grown GaAs and (Al,Ga)As as the system cleans up, following a reload, is reflected in higher values of mobility for 2DEG structures. The dependence of the mobility on the structural parameters of the device can be qualitatively understood as resulting from a combination of scattering processes, i.e. by remote and background impurities, and by acoustic phonons. Quantitative comparison with theory, however, shows that, in general, the experimentally observed mobilities are significantly higher than expected, even when a more realistic model, involving surface depletion and deep and shallow impurity levels, is used.

Acknowledgements - We wish to thank J. Hewett and C. White for their technical assistance, and G. Duggan and J.W. Orton for helpful discussions.

## 7. References

- K. Hess, Appl. Phys. Lett. <u>35</u>, 484 (1979).
- W. Walukiewicz, H.E. Ruda, J. Lagowski and H.C. Gatos, Phys. Rev. B 30, 4571 (1984).

- 3. P.J. Price, Surface Science <u>143</u>, 145 (1984).
- 4. F. Stern, Appl. Phys. Lett. 43, 974 (1983).
- K. Lee, M.S. Shur, T.J. Drummond and H. Morkoc, J. Appl. Phys. 54, 6432 (1983).
- 6. Y. Takeda, H. Kamei and A. Sasaki, Electronics Lett. 18, 311 (1982).
- K. Hirakawa and H. Sakaki, Phys. Rev. B 33, 8291 (1986).
- C.T. Foxon, J.J. Harris, R.G. Wheeler and D.E. Lacklison, J. Vac. Sci. Technology <u>B4</u>, 511 (1986).
- J.J. Harris, C.T. Foxon, K.W.J. Barnham,
   D.E. Lacklison, J. Hewett and C. White,
   submitted to Appl. Phys. Lett. (1986).
- C.T. Foxon and J.J. Harris, Philips J. Res. 41, 313 (1986).
- 11. G.E. Stillman and C.M. Wolfe, Thin Solid Films 31, 69 (1976).
- P. Dawson, G. Duggan, H.I. Ralph and K. Woodbridge, Superlattices and Microstructures <u>1</u>, 173 (1985).
- M. Heiblum, E.E. Mendez and F. Stern, Appl. Phys. Lett. <u>44</u>, 1064 (1984).
- 14. N. Chand, T. Henderson, J. Klem, W.T. Masselink, R. Fischer, Y-C. Chang and H. Morkoç, Phys. Rev. B30, 4481 (1984).
- E.F. Schubert and K. Ploog, Phys. Rev. <u>B30</u>, 7021 (1984).
- K.W.J. Barnham, J.J. Harris, D.E. Lacklison and C.T. Foxon, in preparation.